Supporting Information

Confined Dispersion of Zinc Hydroxystannate Nanoparticles into Layered Bimetallic Hydroxides Nanocapsules and Its Application in Flame Retardant Epoxy Nanocomposites

Zhida Zhang[a], Xueli Li[b], Yongshuai Yuan[a], Ye-Tang Pan[a]*, De-Yi Wang[c], Rongjie Yang[a]

[a] *National Engineering Technology Research Center of Flame Retardant Materials, School of Materials Science & Engineering, Beijing Institute of Technology, Beijing 100081, PR China*

[b] *School of Materials Science & Engineering, Beijing Institute of Technology, Beijing 100081, PR China*

[c] *IMDEA Materials Institute, C/Eric Kandel, 2, 28906 Getafe, Madrid, Spain*

Email: 6120180038@bit.edu.cn

Content of SI

Characterizations

X-ray diffraction (XRD): The X-ray diffraction patterns of the samples were acquired with an X-ray diffractometer (DX-2600, Rigaku corporation, Tokyo, Japan) with a scaned speed of 8°/min from 2° to 40°.

X-ray photoelectron spectroscopy (XPS): The X-ray photoelectron spectroscopy data were gathered on a Perkin-Elmer PHI 5300 ESCA system at 250 W (12.5 kV at 20 mA) under vacuum ($<10^{-6}$ Pa (10^{-8} Torr)). An ion gun and an electronic gun were used to neutralize the sample.

Thermogravimetric analysis (TGA): Thermogravimetric analysis was performed using a NETZSCH 209 F1 thermal analyzer (NETZSCH, Bavarian, Germany) at a heating rate of 20 ℃/min from 40 ℃ to 900 ℃ under nitrogen atmosphere.

Fourier-transform infrared spectroscopy (FT-IR): Fourier-transform infrared spectra with a resolution of 4 cm^{-1} were gathered on a Nicolet 6700 IR spectrometer (BRUKER OPTICS, Beijing, China) by collecting 32 scans with the transmission mode in the range of 4000-400 cm^{-1}.

Scanning electron microscopy (SEM): Scanning electron microscopy was carried out on EVO MA15 Zeiss.

Transmission electron microscopy (TEM): Transmission electron microscopy equipped with energy dispersive X-ray detector (EDX) was operated by a Hitachi-7700 working at 100 kV. The specimens were prepared by dissolving the samples into ethanol, and placed a drop of the solution on a copper grid.

Specific surface area analysis: The specific surface area of all samples was measured

by the BET method on a 3H-2000PS2 analyzer (BeiShiDe Instrument).

Limiting oxygen index test (LOI): The limiting oxygen index was obtained according to the standard ASTM D 2863 procedure by an oxygen index instrument (Rheometric Scientific Ltd., (Phoenix Instruments Co., Ltd, Suzhou, China). And the dimensions of the samples were 125 × 6.5 × 3.2 mm^3.

Vertical burning tests: Vertical burning tests were performed using the UL 94 standard with the CZF-5A horizontal vertical burning tester by Jiangning Analytical Instrument Factory (Phoenix Instruments Co., Ltd, Suzhou, China). And the sheet dimensions were 125 × 13 × 3.2 mm^3.

Cone calorimeter test: Cone calorimeter data were collected by using a Fire Testing Technology apparatus (Phoenix Instruments Co., Ltd, Suzhou, China) with a truncated cone-shaped radiator according to the ISO 5660 protocol. The incident radiant flux is 50 kW/m^2 and the specimen (100 × 100 × 3 mm) was measured horizontally without any grids.

Raman spectroscopy: The Raman spectra data were recorded on a renishaw invia confocal microscopy Raman system with 632.8 nm wavelength laser at ambient temperature.

Differential scanning calorimetry (DSC): Differential scanning calorimetry curves of the EP composites were measured using a Netzsch 204 F1 differential scanning calorimeter (NETZSCH, Bavarian, Germany). The heating rate is 10 ℃/min and the cooling rate is 20 ℃/min. The first heating range was from 20 ℃ to 250 ℃ and the second heating range was from 25 ℃ to 250 ℃.

Dynamic mechanical analysis (DMA): The dynamic mechanical properties of the epoxy nanocomposites were performed in sheer mode with a METTLER TOLEDO SDTA861 instrument (Greifensee, Switzerland). The dimensions of the samples were 6.5 × 6.5 × 3.2 mm^3 and the temperature ramp rate is 10 °C/min from 60 to 240 °C at a frequency of 1.0 Hz.

Mechanical property tests: The mechanical properties were measured with an electronic tensile testing machine (DXLL-5000, Shanghai D & G Measure Instrument Co. Ltd.) at a rate of 2 mm/min.

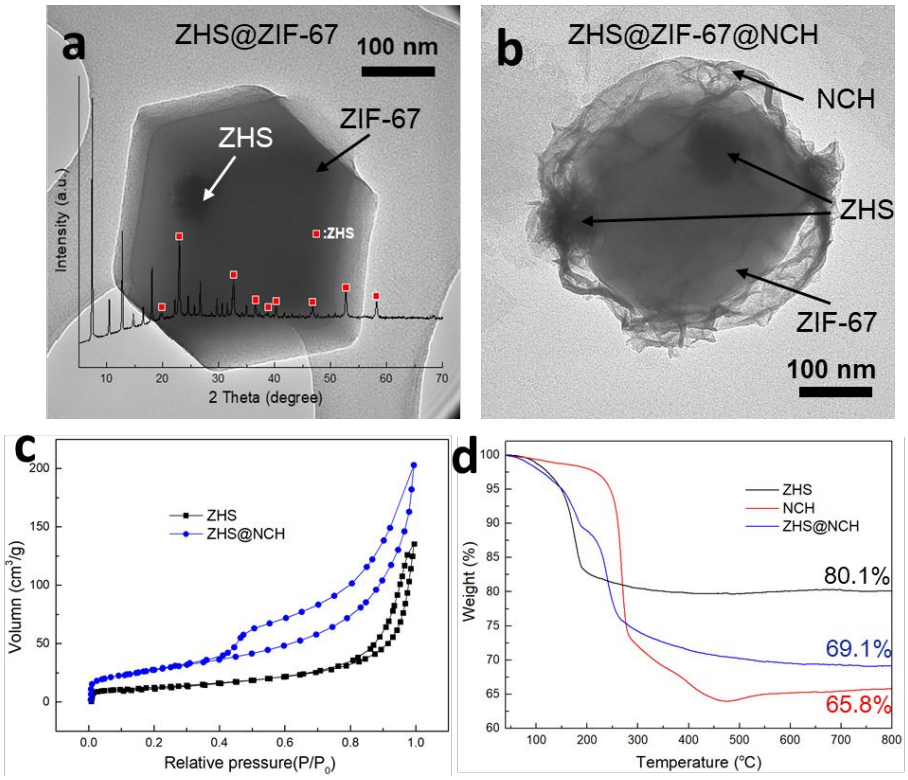

Figure S1. TEM images of (a) intermediate product and (b) product obtained in the etching procedure for the fabrication of hybrid at 20 min; (c) Nitrogen sorption isotherms of ZHS and ZHS@NCH; (d) TGA profiles of ZHS, NCH and ZHS@NCH.

To further survey the evolution process of ZHS@NCH to pave the path for developing more confined-dispersion nanomaterials, TEM images for ZHS@ZIF-67 and the product (ZHS@ZIF-67@NCH) collected during the etching procedure at 20 min were shown in **Figure S1**a and **Figure S1**b, respectively. In ZHS@ZIF-67, ZHS nanocube was inserted into ZIF-67 polyhedron recognized by the different contrast of TEM. The XRD pattern in the inset of **Figure S1**a suggested the overlap of ZHS and ZIF-67 peaks. When the etching procedure for ZIF-67 by nickel salt proceeded after 20 min, the outside surface of ZIF-67 was ablated, and instead, folded NCH nanosheets emerged and formed a yolk-shell nanostructure with the unreacted ZIF-67. The ZHS nanocubes dispersed separately in the yolk part.

The specific surface areas and pore sizes of ZHS and ZHS@NCH were obtained by nitrogen adsorption-desorption isotherms shown in **Figure S1**c. Both isotherms were ascribed to type IV, while hysteresis loop of ZHS was H1, indicating the existence of mesopores with narrow pore size distribution in agreement with the TEM image. The hysteresis loop of ZHS@NCH was H3 mainly attributed to slit hole, demonstrating the layered structure of NCH.

The loading amount is also an important parameter for the hybrid nanomaterials. Herein, we exploited TGA profiles of sample powders (**Figure S1**d) to calculate the loading amount of ZHS in the hybrid. The ZHS curve presented one-step

decomposition due to the loss of OH group; The decomposition of NCH was two step ascribing to the loss of NO_3^- and H_2O in the interlayers followed by the degradation of hydroxides; The hybrid curve was an adduct of ZHS and NCH. On the basis of residue amounts, the weight ratio of ZHS in ZHS@NCH was 23.1%.

Calculation of dead pore rate

We use the following formula to calculate the "dead pore rate" to determine whether the epoxy resin infiltrate the hollow cavity of ZHS@NCH:

$$V = \frac{\frac{1}{\rho} - \frac{1}{\rho(\text{epoxy})}\left(\frac{100 - x}{100}\right) - \frac{1}{\rho(ZHS@NCH)}\left(\frac{x}{100}\right)}{\left(\frac{x}{100}\right)} \quad (1)$$

$$\text{Dead pore ratio}(\%) = \frac{(V_0 - V)}{V_0} \times 100 \quad (2)$$

Here, V_0 is the total pore volume of ZHS@NCH, x is the additive amount ratio of ZHS@NCH in the EP/ZHS@NCH composite, ρ, ρ(epoxy) and ρ(ZHS@NCH) are the specific gravity of the composites. V_0 was measured from the N_2 adsorption isotherm, the density of EP, ZHS@NCH and EP/ZHS@NCH composite were determined by the automatic true density tester.

When all the pores of ZHS@NCH are fully filled with the epoxy resin, the dead pore ratio becomes 100%, while it is 0% if all the pores spaces remain.

By calculation, the dead pore rate is about 94%, indicating that the epoxy matrix have entered the ZHS@NCH nanocages through the mesopores.

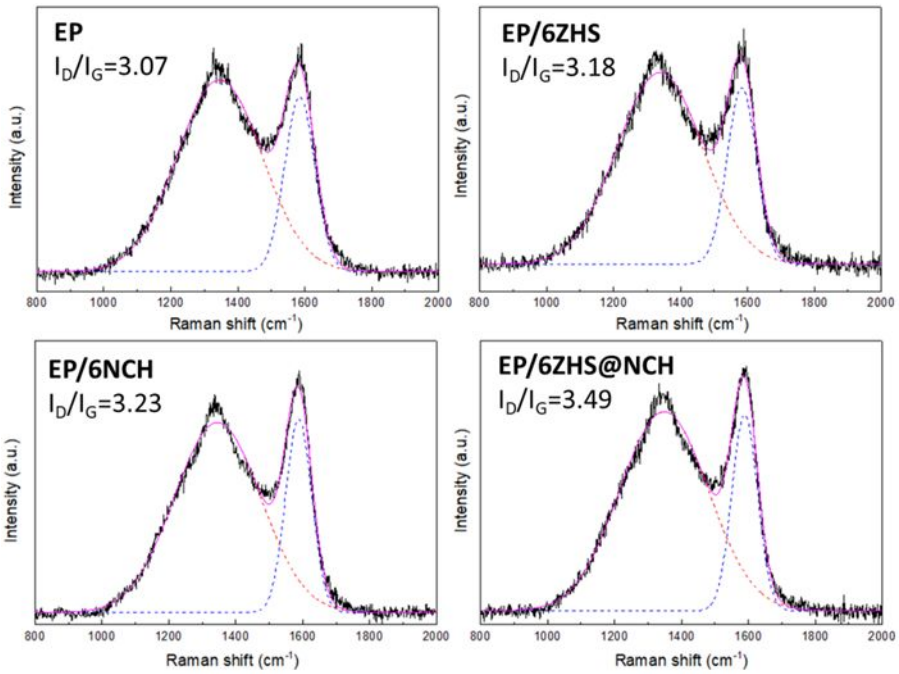

Figure S2. Raman spectra of the char residues of EP and its nanocomposites.

The char residues were further studied by Raman spectra (**Figure S2**). The signal of the D-band (diffusion band around 1350 cm^{-1}) corresponding to sp^3 hybridized C atoms and the G-band (diffusion band around 1350 cm^{-1}) related to the C-C vibrations in aromatic structures could be obviously identified in all of the residue samples.